Hydrogen Isotopes Preclude Marine Hydrate CH4 Emissions at the Onset of Dansgaard-Oeschger Events

Michael Bock, *et al.*

Science **328**, 1686 (2010);
DOI: 10.1126/science.1187651

thousands of kilometers interior to the northern plains retain hydrated silicates. A likely sequence is thus as follows: The bulk of the aqueous alteration of the crust happened after the dichotomy formed but before the onset of volcanic activity that built the Tharsis plateau and contributed to the infilling of the northern plains. The phyllosian environment affected the entire planet during a highly restricted period of time.

References

1. J.-P. Bibring *et al.*, *Eur. Space Agency Spec. Pub.* **1240**, 37 (2004).
2. S. Murchie *et al.*, *J. Geophys. Res.* **114**, E00D07 (2009).
3. J. L. Bandfield, *J. Geophys. Res.* **107**, 5042 (2002).
4. J.-P. Bibring *et al.*, *Science* **307**, 1576 (2005); published online 17 February 2005 (10.1126/science.1108806).
5. P. R. Christensen *et al.*, *Nature* **436**, 504 (2005).
6. F. Poulet *et al.*, *Nature* **438**, 623 (2005).
7. J. F. Mustard *et al.*, *Nature* **454**, 305 (2008).
8. J. Carter *et al.*, *Proc. Lunar Planet. Sci. Conf.* **40**, abstr. 2028 (2009).
9. V. R. Baker *et al.*, *Nature* **352**, 589 (1991).
10. K. L. Tanaka *et al.*, *J. Geophys. Res.* **108**, (E4), 8043 (2003).
11. S. W. Ruff *et al.*, *Icarus* **168**, 131 (2004).
12. M. B. Wyatt, H. Y. McSween Jr., *Nature* **417**, 263 (2002).
13. M.R. Salvatore *et al.*, *Proc. Lunar Planet. Sci. Conf.* **40**, abstr. 2050 (2009).
14. J. F. Mustard *et al.*, *Science* **307**, 1594 (2005); published online 17 February 2005 (10.1126/science.1109098).
15. M. T. Zuber *et al.*, *Science* **287**, 1788 (2000).
16. G. Picardi *et al.*, *Science* **310**, 1925 (2005); published online 30 November 2005 (10.1126/science.1122165).
17. D. Baratoux *et al.*, *J. Geophys. Res.* **112**, E08S05 (2007).
18. M. A. Kreslavsky, J. W. Head, *Meteorit. Planet. Sci.* **41**, 1633 (2006).
19. D. Rogers, P. R. Christensen, *J. Geophys. Res.* **108**, 5030 (2003).
20. K. R. Stockstill-Cahill, F. S. Anderson, V. E. Hamilton, *J. Geophys. Res.* **113**, E07008 (2008).
21. B. Gondet *et al.*, in *Seventh International Conference on Mars*, Lunar and Planetary Institute, Pasadena, CA, 9 to 13 July 2007, abstr. 3185.
22. M. A. Kreslavsky, J. W. Head, *J. Geophys. Res.* **107**, 5121 (2002).
23. M. A. Kreslavsky, J. W. Head, *Geophys. Res. Lett.* **29**, 1719 (2002).
24. J. W. Head, M. A. Kreslavsky, S. Pratt., *J. Geophys. Res.* **107**, 10.1029/2000JE001445 (2002).
25. J. L. Bishop, M. D. Lane, M. D. Dyar, A. J. Brown, *Clay Miner.* **43**, 35 (2008).
26. S. M. Pelkey *et al.*, *J. Geophys. Res.* **112**, E08S14 (2007).
27. J. L. Dickson, C. I. Fassett, J. W. Head, *Geophys. Res. Lett.* **36**, L08201 (2009).
28. M. Frey, D. Robinson, *Low-Grade Metamorphism* (Blackwell, Oxford, 1999).
29. O. Abramov, D. A. Kring, *J. Geophys. Res.* **110**, (E12), E12S09 (2005).
30. J. A. Rathbun, S. W. Squyres, *Icarus* **157**, 362 (2002).
31. S. P. Schwenzer, D. A. Kring, *Geology* **37**, 1091 (2009).
32. B. L. Ehlmann *et al.*, *J. Geophys. Res.* **114**, E00D08 (2009).
33. S. L. Murchie *et al.*, *J. Geophys. Res.* **114**, E00D06 (2009).
34. J.-P. Bibring *et al.*, *Science* **312**, 400 (2006).
35. R. N. Clark *et al.*, U.S. Geological Survey (USGS) Digital Spectral Library splib06a, USGS Digital Data Series 231 (USGS, Denver, CO, 2007).

Supporting Online Material

www.sciencemag.org/cgi/content/full/328/5986/1682/DC1
Figs. S1 and S2

2 March 2010; accepted 20 May 2010
10.1126/science.1189013

Hydrogen Isotopes Preclude Marine Hydrate CH_4 Emissions at the Onset of Dansgaard-Oeschger Events

Michael Bock,[1,2]* Jochen Schmitt,[1,2] Lars Möller,[2] Renato Spahni,[1] Thomas Blunier,[3] Hubertus Fischer[1,2]

The causes of past changes in the global methane cycle and especially the role of marine methane hydrate (clathrate) destabilization events are a matter of debate. Here we present evidence from the North Greenland Ice Core Project ice core based on the hydrogen isotopic composition of methane [$\delta D(CH_4)$] that clathrates did not cause atmospheric methane concentration to rise at the onset of Dansgaard-Oeschger (DO) events 7 and 8. Box modeling supports boreal wetland emissions as the most likely explanation for the interstadial increase. Moreover, our data show that $\delta D(CH_4)$ dropped 500 years before the onset of DO 8, with CH_4 concentration rising only slightly. This can be explained by an early climate response of boreal wetlands, which carry the strongly depleted isotopic signature of high-latitude precipitation at that time.

Rapid stadial-interstadial climate changes during Marine Isotope Stage 3 (MIS3), as recorded in Greenland ice (*1*), had a strong impact around the globe (*2*–*5*). Some of the stadials were accompanied by large discharges of icebergs from the Laurentide ice sheet, known as Heinrich events (*4*). Atmospheric methane concentrations in ice cores show abrupt increases in concert with Dansgaard-Oeschger (DO) warmings (*5*, *6*), although the causes of these methane jumps are not yet unambiguously understood. Preindustrial methane sources include wetlands, thermokarst lakes, ruminants, termites, biomass burning, ultraviolet radiation–induced release by plants, and clathrates (*7*–*11*). Wetlands, the major natural source of atmospheric methane, may be able to respond rapidly enough to changes in temperature and the hydrological cycle to account for the CH_4 increases (*5*, *7*, *12*, *13*). Another hypothesis suggests that the observed rises were due to emissions of marine clathrates stored at the continental margins, which may have been destabilized by a warming of intermediate waters (*14*–*16*). Clathrate destabilization events were indeed found in selected marine sediments (*14*, *17*), although their contribution to the atmospheric budget has been questioned (*5*, *13*, *18*). A change in the CH_4 sink, and thus lifetime, may also have contributed to the observed CH_4 concentration changes.

Methanogenic pathways determine both the carbon and hydrogen isotopic signatures (*8*) of the emitted CH_4, which in turn can be used to better constrain the global methane budget (*9*). Source isotopic compositions may vary as a result of changes in methane precursor material, diffusion and oxidation processes that depend on water table depth in wetlands, or temperature changes in the aerobic zone of tundra soils (*19*). Moreover, the hydrogen isotopic composition of methane [$\delta D(CH_4)$] produced in terrestrial ecosystems is a function of the isotopic signature of precipitation (*8*). The hydrogen isotopic signature of precipitation changed globally because of the temporal variation in the isotopic composition of the ocean, which is a function of the size of polar ice sheets. Schrag *et al.* report δD values of the Last Glacial Maximum (LGM) ocean to be 6.5 to 9 per mil (‰) more enriched than those of today's ocean (*20*). Assuming a maximum sea-level rise of 30 m during DO 8 (*21*), this translates into a hydrogen isotopic shift of the well-mixed ocean of about 2‰. Superimposed on this global change, a stronger Rayleigh distillation effect in meteoric water is expected in high latitudes for cold climate conditions, due to the stronger pole-to-equator temperature gradient. For instance, water isotopes in modeled precipitation suggest that δD_{water} values were 15 to 30‰ lower in northern latitudes during the LGM, whereas values may have been 0 to 8‰ higher in the tropics (*22*).

Rapid changes in the low-latitude hydrological cycle are recorded in marine sediments (*23*), speleothems (*3*, *24*), and leaf waxes in lake

[1]Climate and Environmental Physics, Physics Institute and Oeschger Centre for Climate Change Research, University of Bern, Sidlerstrasse 5, 3012 Bern, Switzerland. [2]Alfred Wegener Institute for Polar and Marine Research, Am alten Hafen 26, 27568 Bremerhaven, Germany. [3]Centre for Ice and Climate, Niels Bohr Institute, University of Copenhagen, Juliane Maries Vej 30, DK-2100 Copenhagen Ø, Denmark.

*To whom correspondence should be addressed. E-mail: bock@climate.unibe.ch

sediments (*25*). These records show latitudinal swings in the Intertropical Convergence Zone (ITCZ), which may have had a strong impact on the local hydrological cycle. In general, little change in δD_{water} is expected close to the ITCZ, where atmospheric water is rapidly recycled. On a global scale, ITCZ swings should therefore lead to a latitudinal relocation of tropical wetlands, but we expect only a secondary effect on the methane hydrogen isotopic signature recorded in ice cores. Changes in the extent of tropical wetlands, which affect the source strength, are difficult to constrain because changes in land area, precipitation patterns, terrain slope, and water-retaining soil layers have to be considered.

Finally, the reaction of CH_4 with the OH radical is the major sink for methane (*9*). The change in kinetic fractionation due to stadial-interstadial temperature changes is limited to less than 3‰ (*18*). We also assume that the relative contributions of the OH, stratospheric, and soil sinks have not substantially changed over time and, therefore, that sink processes have only minor effects on our $\delta D(CH_4)$ record. In summary, we interpret the observed variations in our $\delta D(CH_4)$ time series to be mainly changes in the source mix, with secondary effects of changes in the isotopic composition of precipitation, especially in high latitudes.

Because the hydrogen isotopic composition of methane emitted by marine clathrates (~−190‰) is much heavier than that of the predominant wetland sources (−300 to −400‰) (*18*, *26*), $\delta D(CH_4)$ measurements are well suited to assessing the contribution of marine clathrates to the atmospheric CH_4 budget (*14*). The first $\delta D(CH_4)$ data from an ice core suggested that methane clathrates were stable during the rapid Bølling-Allerød and Younger Dryas–Preboreal warmings (*18*). Furthermore, a complete $\delta^{13}CH_4$ record over the last glacial-interglacial transition (*13*), together with the interhemispheric CH_4 gradient (IHG) (*5*, *27*), showed that boreal wetland CH_4 emissions were essentially shut down during cold stages, and that the atmospheric lifetime of methane was substantially reduced (*13*).

Here we present a high-resolution atmospheric $\delta D(CH_4)$ record (Fig. 1) from the NGRIP ice core spanning DO events 7 and 8, i.e., 33.7 to 41.0 ky B.P. (thousand years before present, where present is defined as 1950 CE). We analyzed 61 samples in randomized order with high precision (±3.4‰), using a technique described previously (*26*, *28*). Over DO 7 and 8, the mean nominal time resolution was 88 years. Reconstructed atmospheric values for $\delta D(CH_4)$ ranged from −77.6 to −98.5‰. In general, we observed higher $\delta D(CH_4)$ for stadial (about −80‰) than interstadial (<−90‰) conditions. This depleted isotopic composition during interstadials precludes a dominant influence of isotopic-enriched clathrate emissions. There are also notable features superimposed that highlight differences between the two investigated DO cycles. In particular, we find a pronounced, 16‰ drop in $\delta D(CH_4)$ that precedes the fast CH_4 increase into DO 8 by ~500 years, in agreement with the few previously published data points from the Greenland Ice Sheet Project 2 (GISP2) ice core (*18*). The drop occurs simultaneously with a slight increase in NGRIP temperatures (*6*) and Greenland ice core CH_4 concentrations [~40 parts per billion by volume (ppbv)] late in the stadial (Fig. 1), at a time when ice rafting debris counts had relaxed from peak Heinrich event conditions (*4*). We propose a slow restart of the Atlantic Meridional Overturning Circulation (AMOC) 500 years before the rapid DO warming in the north. As expected from the bipolar seesaw concept, this would lead to a change in the Southern Ocean warming rate. Although the synchronization error of bipolar ice core records is on the order of 400 years for this interval (*2*) and does not allow a firm conclusion on the exact timing, a change in the warming rate is observed in Antarctic ice cores before the CH_4 increase (*2*). Later during interstadial 8, $\delta D(CH_4)$ rises to stadial levels with two excursions of about +10‰ that occurred at 36.7 and 37.4 ky B.P., i.e., when CH_4 is near its interstadial level and $\delta^{18}O_{ice}$ in the NGRIP ice core is slowly decreasing.

The IHG is small during stadials and large during DO 7 and at the beginning of DO 8, but again reduced at the end of interstadial 8 (*2*). Accordingly, we used the combined information from the IHG and CH_4 isotopes (*26*) to quantify source contributions for three time slices ["stadial," "early-interstadial," and "late-interstadial" (table S1)] using a model approach described previously (*13*). A simple four-box model of the atmosphere was run with prescribed values for CH_4 source strengths, lifetime, and source isotopic compositions in a Monte Carlo approach to constrain our CH_4 budget (*13*, *26*).

An initial estimate constrained only by the ice core records (table S1 and fig. S4) revealed significantly reduced atmospheric lifetimes for both climatic stages compared to the present, with even lower lifetimes during the stadial (4.3 years) compared to both interstadial (4.8 years) runs. For our final best-guess estimate (*26*) (table S2 and fig. S5), we limited our model to lifetimes longer than 5 years (*13*), in line with a three-dimensional chemistry model (*29*). This approach showed a strong reduction of boreal wetland sources during the stadial and an increased contribution in both interstadial scenarios. Moreover, a substantial interstadial increase in marine clathrate emissions can be excluded by our modeled CH_4 budget for both interstadial scenarios. According to our model, the high-latitude wetland emissions strengthened by a factor of 6 (from ~5 to ~32 Tg CH_4 $year^{-1}$) from stadial to early-interstadial conditions, whereas tropical wetland emissions strengthened only moderately for the long interstadial 8 (from ~84 to ~118 Tg CH_4

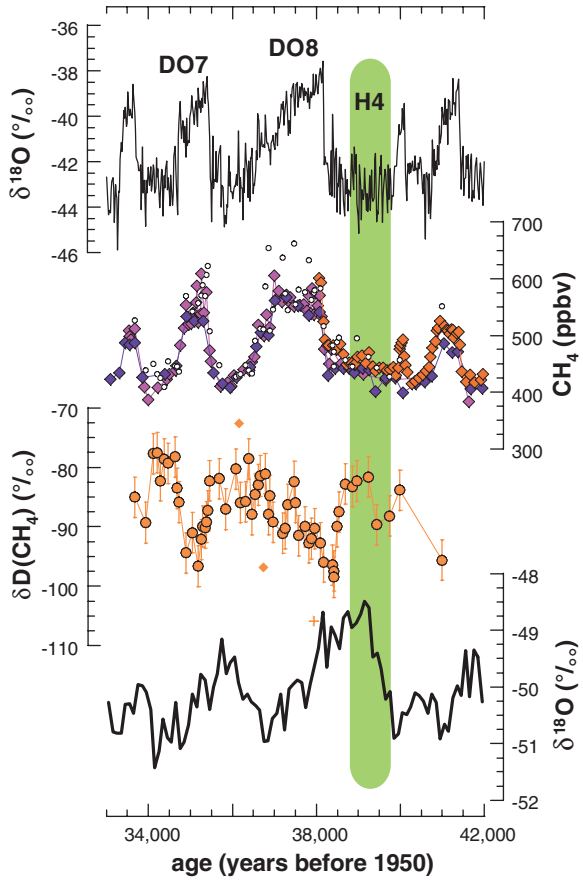

Fig. 1. Stadial and interstadial changes in temperature proxies, CH_4 and $\delta D(CH_4)$. Top and bottom panels show the temperature proxy $\delta^{18}O_{ice}$ from NGRIP (*1*) and the European Project for Ice Coring in Antarctica ice core from Dronning Maud Land (EDML) (*2*), respectively. The second panel shows CH_4 records from GRIP (Greenland Ice Core Project) (purple diamonds), NGRIP (orange diamonds) [(*2*) and this study (open circles), but the latter with much lower precision due to a higher error in determining the total air content)], and EDML (blue diamonds) (*2*). $\delta D(CH_4)$ values in the third panel are from the NGRIP ice core (orange circles) (this study) with a precision of 3.4‰. All data sets are given on the NGRIP GICC05 age scale after CH_4 synchronization. The green bar indicates the Heinrich 4 event (H4). Two $\delta D(CH_4)$ samples (orange diamonds) were excluded from the data set due to technical problems, and one sample (orange cross) was rejected as the gas enclosure process in ice precludes a jump of this size within less than 1 m [for further details, see (*26*)].

year^{-1}). Biomass-burning emissions showed slightly higher values during the interstadial time slices (~55 to 60 versus ~45 Tg CH_4 year^{-1} in the stadial), and marine hydrate emissions were rather constant at ~25 Tg CH_4 year^{-1}. Recent work has shown that other geologic CH_4 emissions may also play a greater role than previously assumed (*30*). Incorporating a geologic source in our model with $\delta D(CH_4)$ in the same range as clathrates and $\delta^{13}CH_4$ between wetlands and biomass burning (*8*) would reduce emission estimates from both biomass burning and clathrates.

To assess the drop in $\delta D(CH_4)$ observed before the onset of DO 8, we ran our model in a transient mode (Fig. 2, left panels). We could not reproduce the strong drop in $\delta D(CH_4)$ along with the small CH_4 concentration rise by strengthening a single source only (*26*). We ran the model with the stadial best-guess setting and forced it with 3.2 times higher boreal emissions (19 Tg CH_4 year^{-1}) and 10% higher tropical wetland emissions to explain both the $\delta D(CH_4)$ and IHG changes. Moreover, we also had to lower the hydrogen isotopic signatures of the boreal source by 30‰ and the tropical source by 5‰ to achieve the drop in $\delta D(CH_4)$ without violating the IHG constraint. Such a lowering of the boreal wetland $\delta D(CH_4)$ seems to be justified in view of the strongly depleted δD signature of high-latitude precipitation and snow melt during cold stadial conditions (*26*). An alternative explanation for this massive isotopic effect may be an increase in net to gross CH_4 production in wetlands (*18*), with net emissions increasing slightly. Global vegetation modeling including CH_4 emissions and isotopes may clarify this issue in the future.

In a second transient model run, we assessed the possibility of marine clathrates contributing to the two positive excursions lasting ~300 years with an amplitude of ~10‰ in $\delta D(CH_4)$ during interstadial 8 (Fig. 1), where evidence for local clathrate destabilization events had been found in marine sediments (*17*). To constrain $\delta D(CH_4)$, we ran the model with the late-interstadial best-guess setting, superimposed with a clathrate CH_4 injection of 20 Tg CH_4 year^{-1} for 250 years, as estimated by (*17*) (Fig. 2, right panels). Such a scenario can explain the observed increase in δD (CH_4), but would require a concurrent increase in CH_4 concentration by ~42 ppbv (Fig. 2). Although this is not supported by currently available CH_4 concentration data, it cannot be entirely ruled out, owing to their insufficient precision and temporal resolution (*2*).

Explanations that alter $\delta D(CH_4)$ but keep the total methane flux constant are more attractive. A synchronous reduction in wetland methane emissions when clathrates are strengthening would be coincidental, as no causal connection between the two exists. However, biomass burning might be opposite in phase with wetland CH_4 emission changes (*31*), thus replacing a depleted wetland with an enriched biomass-burning source. Again, changes in the net to gross CH_4 production from wetlands would shift atmospheric $\delta D(CH_4)$ to heavier values when gross production increases while the net flux stays constant (*18*). Analogously, this could explain the slow rise in $\delta D(CH_4)$ during DO 8 in parallel to an increasingly colder and drier climate. Alternatively, short-term changes in δD in high-latitude precipitation could contribute to the positive excursions without affecting boreal emission strength. NGRIP and EDML $\delta^{18}O_{ice}$ show temperature variations in the course of the interstadial; however, uncertainties in the ice age–gas age difference do not allow us to unambiguously synchronize temperature and CH_4 variations.

Even though the methane cycle is still underdetermined, our measurements show that marine hydrate destabilization did not occur at the end of stadials, and if it occurred at all, then only intermittently in the course of interstadials, when the surface warming had propagated to intermediate depths in the ocean. In contrast, our isotopic budget is consistent with the idea that wetlands were the main drivers of short- and longer-term CH_4 concentration variations in the past. In addition to changes in the source mix, our hydrogen isotopic signature of atmospheric methane appears to be affected by changes in δD of precipitation in high latitudes. In our $\delta D(CH_4)$ data, we find clear evidence for a climate response in boreal wetland regions that precedes the rapid warming into DO 8. This has implications for the timing of the trigger for the DO 8 warming and suggests that the AMOC is already slowly recovering in the preceding stadial.

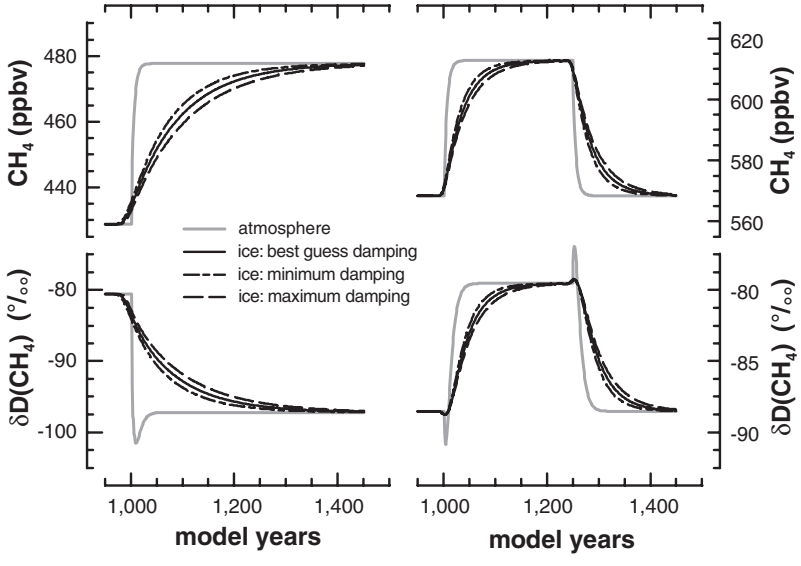

Fig. 2. Transient model response to rapid emission changes. Transient model runs were used to assess the timing and amplitude of simultaneous concentration changes along with observed δD (CH_4) variations. Concentrations (top panels) and $\delta D(CH_4)$ (bottom panels) for the "early boreal wetland" simulation (left panels) and the "clathrate destabilization event" (right panels). We assume a sudden increase in CH_4 emissions. The corresponding atmospheric peak (gray line) was filtered using ice core gas age distributions (black lines) calculated with a diffusion model (*26*) to account for the low-pass filtering effect of the bubble enclosure process (fig. S1). Overshooting of the atmospheric $\delta D(CH_4)$ signal is due to an imbalance in the source and sink composition. We made use of three different age distributions to assess model uncertainties. The stadial gas enclosure characteristic (stronger damping) and the interstadial gas enclosure characteristic (weaker damping) are preferred for the boreal wetland and clathrate simulations, respectively. For the clathrate destabilization, in total 5000 Tg CH_4 with $\delta^{13}CH_4 = -60‰$ and $\delta D(CH_4) = -190‰$ were added in 250 years.

References and Notes

1. North Greenland Ice Core Project members, *Nature* **431**, 147 (2004).
2. EPICA Community Members, *Nature* **444**, 195 (2006).
3. S. J. Burns, D. Fleitmann, A. Matter, J. Kramers, A. A. Al-Subbary, *Science* **301**, 1365 (2003).
4. L. de Abreu, N. J. Shackleton, J. Schönfeld, M. Hall, M. Chapman, *Mar. Geol.* **196**, 1 (2003).
5. E. J. Brook, S. Harder, J. Severinghaus, E. J. Steig, C. M. Sucher, *Global Biogeochem. Cycles* **14**, 559 (2000).
6. C. Huber *et al.*, *Earth Planet. Sci. Lett.* **243**, 504 (2006).
7. G. M. MacDonald *et al.*, *Science* **314**, 285 (2006).
8. M. J. Whiticar, in *Atmospheric Methane: Sources, Sinks, and Role in Global Change*, M. A. K. Khalil, Ed. (Springer, Berlin, 1993), pp. 138–167.
9. P. Quay *et al.*, *Global Biogeochem. Cycles* **13**, 445 (1999).
10. F. Keppler, J. T. G. Hamilton, M. Brass, T. Röckmann, *Nature* **439**, 187 (2006).
11. K. M. Walter, M. E. Edwards, G. Grosse, S. A. Zimov, F. S. Chapin III, *Science* **318**, 633 (2007).
12. J. Chappellaz *et al.*, *Nature* **366**, 443 (1993).
13. H. Fischer *et al.*, *Nature* **452**, 864 (2008).
14. J. P. Kennett, K. G. Cannariato, I. L. Hendy, R. J. Behl, *Methane Hydrates in Quaternary Climate Change: The Clathrate Gun Hypothesis*, B. Jean-Luis, Ed. (AGU Special Publication, Vol. 54, 2003).

15. "Clathrates" hereafter refers to those in intermediate depth, whereas shallow hydrates in (submerged) permafrost are considered to be part of the boreal terrestrial source.
16. E. G. Nisbet, J. Chappellaz, *Science* **324**, 477 (2009).
17. T. de Garidel-Thoron, L. Beaufort, F. Bassinot, P. Henry, *Proc. Natl. Acad. Sci. U.S.A.* **101**, 9187 (2004).
18. T. Sowers, *Science* **311**, 838 (2006).
19. I. Levin, in *Carbon Cycling in the Glacial Ocean: Constraints on the Ocean's Role in Global Change*, R. Zahn et al., Eds. (NATO ASI Series I17, Springer, Berlin, 1994), pp. 1–6.
20. D. P. Schrag *et al.*, *Quat. Sci. Rev.* **21**, 331 (2002).
21. M. Siddall *et al.*, *Nature* **423**, 853 (2003).
22. J. Jouzel, G. Hoffmann, R. D. Koster, V. Masson, *Quat. Sci. Rev.* **19**, 363 (2000).
23. L. C. Peterson, G. H. Haug, K. A. Hughen, U. Röhl, *Science* **290**, 1947 (2000).
24. X. Wang *et al.*, *Nature* **432**, 740 (2004).
25. J. E. Tierney *et al.*, *Science* **322**, 252 (2008).
26. Materials and methods are available as supporting material on *Science* Online.
27. A. Dällenbach *et al.*, *Geophys. Res. Lett.* **27**, 1005 (2000).
28. M. Bock *et al.*, *Rapid Commun. Mass Spectrom.* **24**, 621 (2010).
29. J. Lelieveld, P. J. Crutzen, F. J. Dentener, *Tellus B Chem. Phys. Meterol.* **50**, 128 (1998).
30. G. Etiope, A. V. Milkov, *Environ. Geol. (Berl.)* **46**, 997 (2004).
31. P. Bergamaschi *et al.*, *J. Geophys. Res.* **114**, D22301 (2009).
32. We thank I. Levin for providing a reference air tank along with calibrated isotope values. We thank T. Sowers and two anonymous reviewers for carefully reviewing the manuscript. Financial support for this study was provided in part by the German Secretary of Education and Research program GEOTECHNOLOGIEN, by Deutsche Forschungsgemeinschaft (DFG project MEPHISTO), Schweizerischer Nationalfonds (SNF project *prime*METHANE), and the European Research Council advanced grant MATRICs. This work is a contribution to the North-GRIP ice core project, which is directed and organized by the Department of Geophysics at the Niels Bohr Institute for Astronomy, Physics and Geophysics, University of Copenhagen. It is supported by funding agencies in Denmark (SNF), Belgium (FNRS-CFB), France (IFRTP and INSU/CNRS), Germany (AWI), Iceland (RannIs), Japan (MEXT), Sweden (SPRS), Switzerland (SNF), and the United States (NSF).

Supporting Online Material

www.sciencemag.org/cgi/content/full/328/5986/1686/DC1
Materials and Methods
Figs. S1 to S5
Tables S1 to S3
References and Notes

28 January 2010; accepted 19 May 2010
10.1126/science.1187651

ATP-Binding Cassette Transporters and HDL Suppress Hematopoietic Stem Cell Proliferation

Laurent Yvan-Charvet,[1]*† Tamara Pagler,[1]* Emmanuel L. Gautier,[2] Serine Avagyan,[2] Read L. Siry,[1] Seongah Han,[1] Carrie L. Welch,[1] Nan Wang,[1] Gwendalyn J. Randolph,[2] Hans W. Snoeck,[2] Alan R. Tall[1]

Elevated leukocyte cell numbers (leukocytosis), and monocytes in particular, promote atherosclerosis; however, how they become increased is poorly understood. Mice deficient in the adenosine triphosphate–binding cassette (ABC) transporters ABCA1 and ABCG1, which promote cholesterol efflux from macrophages and suppress atherosclerosis in hypercholesterolemic mice, displayed leukocytosis, a transplantable myeloproliferative disorder, and a dramatic expansion of the stem and progenitor cell population containing $Lin^{-}Sca\text{-}1^{+}Kit^{+}$ (LSK) in the bone marrow. Transplantation of *Abca1*$^{-/-}$ *Abcg1*$^{-/-}$ bone marrow into apolipoprotein A-1 transgenic mice with elevated levels of high-density lipoprotein (HDL) suppressed the LSK population, reduced leukocytosis, reversed the myeloproliferative disorder, and accelerated atherosclerosis. The findings indicate that ABCA1, ABCG1, and HDL inhibit the proliferation of hematopoietic stem and multipotential progenitor cells and connect expansion of these populations with leukocytosis and accelerated atherosclerosis.

Leukocytosis and monocytosis are risk factors for coronary heart disease (CHD) and probably have a causal relationship to this disorder (*1*). In contrast, plasma high-density lipoprotein (HDL) levels are inversely correlated with the incidence of CHD (*2*); however, this observation has not been linked to leukocytosis. The athero-protective effect of HDL is mediated in part by promotion of cholesterol efflux from macrophage foam cells in atherosclerotic lesions (*3*–*5*). Two adenosine triphosphate–binding cassette (ABC) transporters, ABCA1 and ABCG1, play a key role in promoting cholesterol efflux from macrophages to lipid-poor apolipoprotein A-1 (apoA-1) and HDL, respectively. Deletion of *Abca1* and *Abcg1* in mice led to additive defects in macrophage cholesterol efflux and reverse cholesterol transport (*6*, *7*) and accelerated atherosclerosis in a susceptible hypercholesterolemic background (*6*). *Abca1*$^{-/-}$ *Abcg1*$^{-/-}$ mice also showed marked leukocytosis and infiltration of various organs with macrophage foam cells (*6*, *8*–*10*). This led us to hypothesize that these changes might arise, from either an inflammatory response mediated by excessive signaling of Toll-like receptors (TLRs) (*10*) or an excessive proliferation of bone marrow (BM) myeloid cells.

Six-week-old, chow-fed *Abca1*$^{-/-}$ *Abcg1*$^{-/-}$ mice developed increased myeloid cells ($Gr\text{-}1^{high}$ $CD11b^{high}$), monocytosis, and neutrophilia in blood and BM (fig. S1, A and B) (*11*). Blood counts indicated monocytosis, neutrophilia, and eosinophilia (fig. S1C) but normal T and B cell numbers (fig. S1C) and normal hematocrit and platelet counts. Consuming a high-fat diet further increased the peripheral leukocyte and monocyte counts with a balanced increase in "inflammatory" Ly-$6C^{high}$ and "patrolling" Ly-$6C^{low}$ monocyte subsets in *Abca1*$^{-/-}$ *Abcg1*$^{-/-}$ mice, but not in wild-type (WT) mice (figs. S1C and S2). Besides leukocytosis, 12-week-old *Abca1*$^{-/-}$ *Abcg1*$^{-/-}$ mice fed a chow diet developed hepato-splenomegaly and hypertrophy of intestinal Peyer's patches with a cellular infiltrate of macrophage foam cells (*6*, *9*) and neutrophils (fig. S3).

To determine if leukocytosis in *Abca1*$^{-/-}$ *Abcg1*$^{-/-}$ mice might represent an inflammatory response, we bred *Abca1*$^{-/-}$ *Abcg1*$^{-/-}$ to *MyD88*$^{-/-}$ mice, which lack the adapter molecule MyD88 necessary for signaling downstream of some TLRs. These animals showed only slight reductions in leukocyte and neutrophil counts compared with *Abca1*$^{-/-}$ *Abcg1*$^{-/-}$ mice, although spleen weight was similar (fig. S4, A and B). Furthermore, treatment of *Abca1*$^{-/-}$ *Abcg1*$^{-/-}$ mice with broad spectrum antibiotics to suppress potential TLR-dependent responses to the endogenous intestinal flora (*12*) did not reverse leukocytosis or splenomegaly in *Abca1*$^{-/-}$ *Abcg1*$^{-/-}$ mice (fig. S4, C and D). These findings were inconsistent with the hypothesis that leukocytosis represented a TLR/MyD88-dependent inflammatory response.

The phenotype of the *Abca1*$^{-/-}$ *Abcg1*$^{-/-}$ mice suggested a myeloproliferative disorder, and both ABCA1 and ABCG1 are highly expressed in hematopoietic stem and multipotential progenitor cells (HSPCs) (*13*, *14*). Thus, we quantified BM HSPCs and other myeloid populations in chow-fed animals (Fig. 1) (*15*). Remarkably, the $Lin^{-}Sca^{+}cKit^{+}$ (LSK) population representing HSPCs showed a fivefold increase in both frequency and number in *Abca1*$^{-/-}$ *Abcg1*$^{-/-}$ BM (Fig. 1A and fig. S5, A to D). Although the common lymphoid progenitor (CLP) population was unchanged, the granulocyte-monocyte progenitor (GMP) and the common myeloid progenitor (CMP) numbers were increased up to 100% in *Abca1*$^{-/-}$ *Abcg1*$^{-/-}$ BM compared with WT BM (Fig. 1A and fig. S5, E and F). Analysis of different populations within the LSK cells showed

[1]Division of Molecular Medicine, Department of Medicine, Columbia University, New York, NY 10032, USA. [2]Department of Gene and Cell Medicine, Mount Sinai School of Medicine, New York, NY 10029, USA.

*These authors contributed equally to this work.
†To whom correspondence should be addressed. E-mail: ly2159@columbia.edu